

# Diketopyrrolopyrrole–Diketopyrrolopyrrole-Based Conjugated Copolymer for High-Mobility Organic Field-Effect Transistors

Catherine Kanimozhi,<sup>†</sup> Nir Yaacobi-Gross,<sup>‡</sup> Kang Wei Chou,<sup>§</sup> Aram Amassian,<sup>§</sup> Thomas D. Anthopoulos,<sup>\*,‡</sup> and Satish Patil<sup>\*,†</sup>

<sup>†</sup>Solid State and Structural Chemistry Unit, Indian Institute of Science, Bangalore 560012, India

<sup>‡</sup>Department of Physics and Centre for Plastic Electronics, Blackett Laboratory, Imperial College London, London SW7 2BW, U.K.

<sup>§</sup>Physical Sciences and Engineering Division, King Abdullah University of Science and Technology (KAUST), Thuwal 23955-6900, Saudi Arabia

## S Supporting Information

**ABSTRACT:** In this communication, we report the synthesis of a novel diketopyrrolopyrrole–diketopyrrolopyrrole (DPP–DPP)-based conjugated copolymer and its application in high-mobility organic field-effect transistors. Copolymerization of DPP with DPP yields a copolymer with exceptional properties such as extended absorption characteristics (up to  $\sim 1100$  nm) and field-effect electron mobility values of  $>1$  cm<sup>2</sup> V<sup>-1</sup> s<sup>-1</sup>. The synthesis of this novel DPP–DPP copolymer in combination with the demonstration of transistors with extremely high electron mobility makes this work an important step toward a new family of DPP–DPP copolymers for application in the general area of organic optoelectronics.

Ambipolar organic field-effect transistors (OFETs) based on  $\pi$ -conjugated polymers are of interest for complementary-like electronic circuits.<sup>1–5</sup> For this reason, a number of research groups in recent years have focused their efforts on the development of a range of high-performance conjugated polymers with p-type,<sup>6</sup> n-type, and ambipolar properties.<sup>7–10</sup> Among these materials, diketopyrrolopyrrole (DPP)-based conjugated copolymers have been extensively investigated.<sup>11–14</sup>

The electron-deficient nature of DPP, its planar backbone, and intermolecular hydrogen bonding result in materials with strong  $\pi$ – $\pi$  stacking interactions.<sup>15</sup> Such solid-state packing is desired to obtain high-performance OFETs for use in electronic circuits.<sup>16–20</sup> DPP-based conjugated copolymers are prepared by carbon–carbon (Suzuki or Stille) coupling reactions with various comonomers.<sup>12,21–24</sup> The properties of the comonomers strongly influence the performance of these materials in both organic photovoltaic (OPV) and OFET applications. Among these materials, benzothiadiazole (BDT)–DPP has attracted much attention because of its potentially high ambipolar charge carrier mobilities in OFET devices.<sup>11</sup> The electron-deficient BDT unit extends the conjugation and also promotes delocalization of the electron density along the backbone of the copolymer, which results in an enhancement of intermolecular charge hopping. However, the BDT–DPP copolymer is insoluble (high-molecular-weight fraction) in many organic solvents because of the lack of solubilizing groups on the BDT unit.

This early work motivated us to design polymers that contain only DPP chains. The strong intermolecular donor–acceptor interactions between DPP units promote self-assembly of the polymer, which in turn leads to excellent charge transport. In addition, the solubilizing alkyl chain on every DPP unit eliminates the solubility problem. These favorable characteristics of the DPP–DPP copolymer make it promising for application in high-performance OFETs and OPVs. In addition, we engineered the side chains on the DPP unit to allow optimized chain packing and formation of large crystalline domains in the solid state. One of the DPP units functionalized with triethylene glycol (TEG) side chains was found to induce spontaneous chain crystallization while providing maximum solubility, allowing the synthesis of high-molecular-weight DPP–DPP copolymers. Carefully engineered top-gate OFETs based on the TEG-functionalized DPP–DPP copolymer exhibited a maximum electron mobility of 3 cm<sup>2</sup> V<sup>-1</sup> s<sup>-1</sup>. The combination of high carrier mobility and extended absorption up to 1100 nm makes this DPP–DPP copolymer an excellent candidate for use in high-performance (opto)-electronic devices.

The monomers and polymer were synthesized using reactions analogous to procedures reported in the literature<sup>25,26</sup> [synthesis details are provided in the Supporting Information (SI)]. The synthetic scheme for the copolymer N-CS2DPP-OD-TEG is shown in Figure 1. The Suzuki coupling polymerization between 3,6-bis(5-(4,4,5,5-tetramethyl-1,3,2-dioxaborolan-2-yl)thiophen-2-yl)-*N,N*-bis(2-octyldodecyl)-1,4-dioxopyrrolo[3,4-*c*]pyrrole and 3,6-bis(5-bromothiophen-2-yl)-*N,N*-bis(2-(2-(2-methoxyethoxy)ethoxy)ethyl)-1,4-dioxopyrrolo[3,4-*c*]pyrrole was carried out in the presence of the palladium catalyst Pd<sub>2</sub>(DBA)<sub>3</sub> (DBA = dibenzylideneacetone) and the active ligand P(*o*-tol)<sub>3</sub>. The copolymer was purified by precipitation in methanol followed by Soxhlet extraction using methanol, acetone, and hexane, which ensured removal of catalytic impurities and undesired low-molecular-weight oligomers. Finally, reprecipitation in methanol gave a dark-green solid in high yield (70.4%). N-CS2DPP-OD-TEG is highly soluble in most of the common organic solvents (e.g., chloroform, toluene, and tetrahydrofuran) at room temper-

Received: August 18, 2012

Published: September 28, 2012

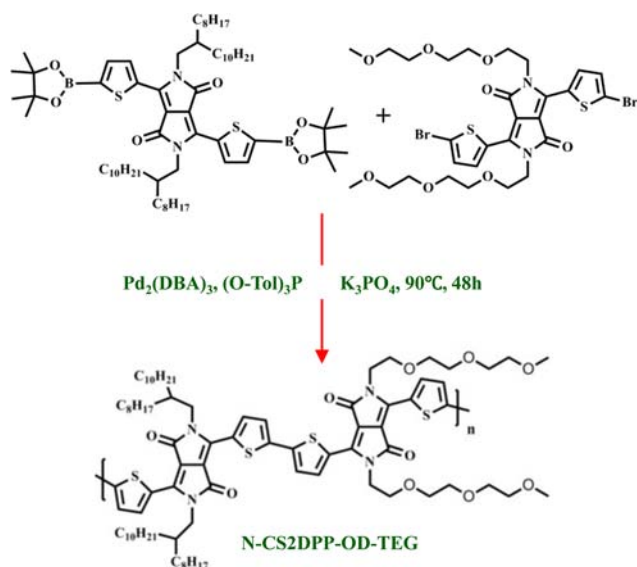


**Figure 1.** Synthesis of N-CS2DPP-OD-TEG by Suzuki coupling reaction.

ature. Gel permeation chromatography (GPC) studies showed a number-average molecular weight of 67.3 kg/mol and a weight-average molecular weight of 314.0 kg/mol with a polydispersity of 4.66.

The UV–vis absorption spectrum of N-CS2DPP-OD-TEG in chloroform exhibited a strong absorption band with a maximum in the near-IR region at  $\sim 900$  nm (Figure S2 in the SI). The thin-film absorption spectrum showed a red shift of 45 nm relative to the solution state, which was attributed to strong solid-state packing and intermolecular interactions. Both the solid-state and solution absorption spectra showed the onset of absorption to occur at  $\sim 1000$  nm, which implies the presence of long-range order or intermolecular interactions in both solution and the solid state. The optical band gap obtained from the solid-state absorption onset was  $\sim 1.2$  eV. Such low-band-gap polymers and oligomers have been found to enhance intramolecular charge transfer, which in turn improves the charge carrier mobility.<sup>27–32</sup> Frontier molecular orbital energy levels were calculated from cyclic voltammetry (CV) (Figure S5). Platinum electrodes were used as the working and counter electrodes, while Ag/Ag<sup>+</sup> was employed as a reference electrode. Energy levels were calculated with respect to an internal-standard ferrocene/ferrocenium (Fc/Fc<sup>+</sup>) redox couple. We found an onset oxidation potential of 0.88 V and an onset reduction potential of  $-0.84$  V, which correspond to a highest occupied molecular orbital (HOMO) of  $\sim 5.38$  eV and a lowest unoccupied molecular orbital (LUMO) of  $\sim 3.66$  eV with respect to the Fc internal standard ( $E_{\text{HOMO}} = 4.80$  eV). The band gap calculated from the electrochemical measurements showed a difference of 0.51 eV relative to the optical band gap, which can be corrected using the exciton binding energy. Thermogravimetric analysis of N-CS2DPP-OD-TEG showed a decomposition temperature of 373 °C (Figure S1), which implies high thermal stability of this polymer.

All of the quantum-chemical calculations were carried out using density functional theory (DFT) with the B3LYP hybrid functional and the 6-31G(d+)\* basis set as implemented in Gaussian 03. After the optimization of the geometrical structures, time-dependent DFT (TDDFT) calculations were performed. Polymer repeating units were used in the TDDFT

calculations, which are useful for predicting the trends in the ground and excited state MO energy levels of conjugated copolymers. The position and optimized electron delocalization of the HOMO and LUMO were calculated using TDDFT and are depicted in Figure 2. The predicted HOMO and LUMO

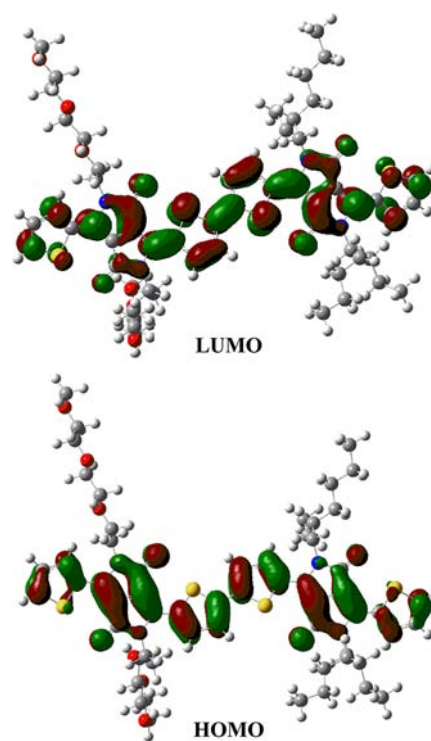


**Figure 2.** Optimized electron delocalization MO diagram of the polymer repeating units.

show similar distributions of electrons throughout their donor (thiophene) and acceptor (DPP) cores. The strong electron donation from the thiophene to the DPP results in strong intramolecular charge transfer and the two thiophene rings have a torsion angle of only  $2^\circ$  tilted from the planar geometry. This prevents the polymer chain from flipping away from its planar geometry, giving an extended conjugation throughout the chain and hence resulting in complete delocalization of the electrons in the LUMO. This repeating unit model represents a polymer chain in which the possibility of transport of both types of charge (electrons and holes) is highly feasible. This type of donor–acceptor polymer has been found to yield high-mobility ambipolar OFETs.<sup>35</sup>

The ordering of the as-spun N-CS2DPP-OD-TEG thin film was evaluated using grazing-incidence X-ray diffraction (GIXRD), and the scattering pattern is shown in Figure 3a. The polymer adopts a common lamellar structure with lamellae parallel to the surface. A lamellar  $d$  spacing of 2 nm was derived from the first-order (100) peak, with a coherence length of 9.1 nm. The  $\pi$ – $\pi$  stacking (010) peak has an associated  $d$  spacing of 0.36 nm and a coherence length of 3.4 nm.

Organic OFETs were fabricated using previously published methods.<sup>34,35</sup> In brief, bottom-gate–bottom-contact (BG–BC) transistors were fabricated using heavily doped silicon wafers as the back gate electrode with a 200 nm thermally oxidized SiO<sub>2</sub> layer as the gate dielectric. Gold source and drain electrodes were then defined using conventional photolithography. Titanium was used as an adhesion layer (10 nm) for the gold

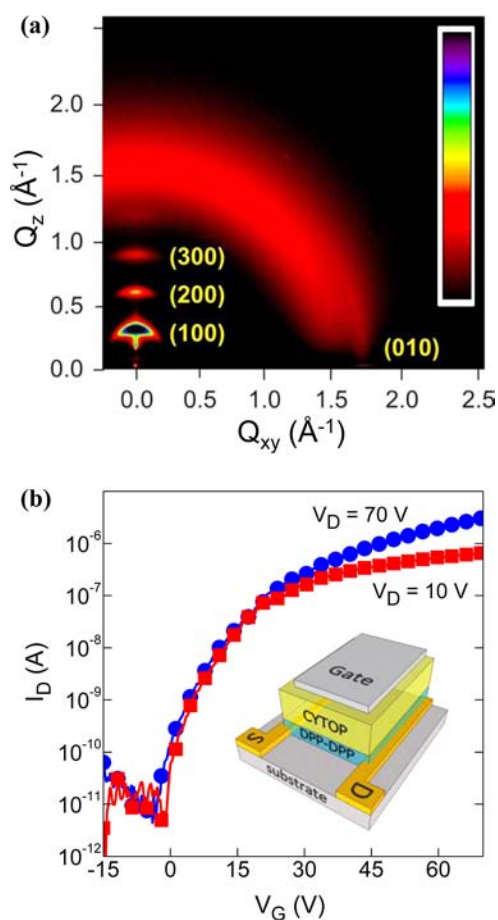


**Figure 3.** (a) GIXRD pattern for the as-spun N-CS2DPP-OD-TEG thin film, exhibiting four orders of lamellar Bragg sheets and an in-plane Bragg peak associated with  $\pi$ - $\pi^*$  stacking. (b) Transfer characteristics of the top-gate–bottom-contact (TG–BC) transistors. The inset shows a schematic of the TG–BC transistor architecture used.

on the SiO<sub>2</sub>. Passivation of the SiO<sub>2</sub> layer was achieved by treating its surface with the primer hexamethyldisilazane. The polymer semiconductor was then spun on top of the substrates to complete the transistor fabrication, and the transistor was thermally annealed at 140 °C in nitrogen. Top-gate–bottom-contact (TG–BC) transistors<sup>35</sup> were fabricated on glass using thermally evaporated 30 nm thick Al or Au source and drain contacts. The polymer solution was spin-coated in nitrogen at 800 rpm for 60 s. The samples were then annealed at 100 °C to dry. A 900 nm thick CYTOP (Ashai Glass) layer acting as the gate dielectric was spin-cast directly onto the polymer semiconductor layer and annealed at 100 °C for 15 min before Al gate electrodes were deposited by thermal evaporation under high vacuum. Device fabrication and characterization was performed in nitrogen.

BG–BC transistors based on N-CS2DPP-OD-TEG exhibited clear ambipolar transport (Figure S7) with balanced electron and hole mobilities in the order of  $\sim 0.01$  cm<sup>2</sup> V<sup>-1</sup> s<sup>-1</sup>. In an effort to improve the charge transport characteristics of N-CS2DPP-OD-TEG transistors, but most importantly to assess the true potential of this novel DPP–DPP copolymer, we realized TG–BC transistors fabricated using previously published methods<sup>35</sup> employing Al as the source and drain electrodes. The TG–BC device architecture is known to yield high-mobility OFETs mainly because of the formation of a

high-quality interface between the organic semiconductor and the fluoropolymer CYTOP dielectric.<sup>35</sup> Figure 3b displays a representative set of transfer characteristics for a top-gate N-CS2DPP-OD-TEG transistor measured under a nitrogen atmosphere. The Figure 3b inset shows a schematic of the transistor structure. The devices showed high channel currents as a direct result of the high electron mobility, which in some “hero” devices exceeded 3 cm<sup>2</sup> V<sup>-1</sup> s<sup>-1</sup>. The channel current on/off ratio was also high, typically in the order of 10<sup>4</sup> or higher. A very interesting observation is that as opposed to the BG–BC transistors (Figure S7), the TG–BC devices showed no hole-transporting characteristics and exhibited strictly unipolar electron accumulation even when the Al source/drain electrodes were replaced with hole-injecting Au ones (i.e., work function  $\sim 5$  eV), as clearly shown in Figure S8. The unipolar n-channel characteristics of the TG–BC devices can be seen as an advantage for applications in printed, low-power, large-scale integrated organic circuits based on complementary logic architectures.

In conclusion, our molecular semiconductor design strategy involving coupling of diketopyrrolopyrrole with diketopyrrolopyrrole in an alternating fashion affords a remarkable improvement in electron mobility. The novel synthetic design approach coupled with the demonstration of organic thin-film transistors with electron mobilities of up to 3 cm<sup>2</sup> V<sup>-1</sup> s<sup>-1</sup> can be seen as an important step toward the development of a new family of high-performance DPP–DPP-based copolymers for use in a wide range of organic (opto)electronic applications.

## ■ ASSOCIATED CONTENT

### 📄 Supporting Information

Materials, experimental details, additional spectra, and device fabrication details. This material is available free of charge via the Internet at <http://pubs.acs.org>.

## ■ AUTHOR INFORMATION

### Corresponding Author

t.anthopoulos@ic.ac.uk; sathish@sscu.iisc.ernet.in

### Notes

The authors declare no competing financial interest.

## ■ ACKNOWLEDGMENTS

The authors acknowledge financial support from the Department of Science and Technology, India through the Indo-UK Apex Program and Ministry of Communication and Information Technology under a grant for the Centre of Excellence in Nanoelectronics, Phase II. We thank our colleagues Dr. Mallari Naik and Dr. N. Venkatramaiah for the TD-DFT calculations and support. We are grateful to Anke Helfer for GPC measurements. T.D.A. and N.Y.G. are grateful to the Engineering and Physical Sciences Research Council (EPSRC) (Grant EP/J001473/1) and the European Research Council (ERC) for financial support. Portions of this research were carried out at the Stanford Synchrotron Radiation Lightsource, a Directorate of SLAC National Accelerator Laboratory and an Office of Science User Facility operated for the U.S. Department of Energy Office of Science by Stanford University.

## ■ REFERENCES

- (1) Chen, J.; Cao, Y. *Acc. Chem. Res.* **2009**, *42*, 1709.



- (2) Sariciftci, N. S.; Smilowitz, L.; Heeger, A. J.; Wudl, F. *Science* **1992**, *258*, 1474.
- (3) Wienk, M. M.; Turbiez, M.; Gilot, J.; Janssen, R. A. J. *Adv. Mater.* **2008**, *20*, 2556.
- (4) Allard, S.; Forster, M.; Souharce, B.; Thiem, H.; Scherf, U. *Angew. Chem., Int. Ed.* **2008**, *47*, 4070.
- (5) Bao, Z.; Lovinger, A. J. *Chem. Mater.* **1999**, *11*, 2607.
- (6) Li, Y.; Singh, S. P.; Sonar, P. *Adv. Mater.* **2010**, *22*, 4862.
- (7) Dallos, T.; Beckmann, D.; Brunklaus, G.; Baumgarten, M. *J. Am. Chem. Soc.* **2011**, *133*, 13898.
- (8) Usta, H.; Newman, C.; Chen, Z.; Facchetti, A. *Adv. Mater.* **2012**, *24*, 3678.
- (9) Fan, J.; Yuen, J. D.; Wang, M.; Seifert, J.; Seo, J.-H.; Mohebbi, A. R.; Zakhidov, D.; Heeger, A.; Wudl, F. *Adv. Mater.* **2012**, *24*, 2186.
- (10) Shahid, M.; McCarthy-Ward, T.; Labram, J.; Rossbauer, S.; Domingo, E. B.; Watkins, S. E.; Stingelin, N.; Anthopoulos, T. D.; Heeney, M. *Chem. Sci.* **2012**, *3*, 181.
- (11) Sonar, P.; Singh, S. P.; Li, Y.; Soh, M. S.; Dodabalapur, A. *Adv. Mater.* **2010**, *22*, 5409.
- (12) Bijleveld, J. C.; Zoombelt, A. P.; Mathijssen, S. G. J.; Wienk, M. M.; Turbiez, M.; de Leeuw, D. M.; Janssen, R. A. J. *J. Am. Chem. Soc.* **2009**, *131*, 16616.
- (13) Bronstein, H.; Chen, Z.; Ashraf, R. S.; Zhang, W.; Du, J.; Durrant, J. R.; Shakya Tuladhar, P.; Song, K.; Watkins, S. E.; Geerts, Y.; Wienk, M. M.; Janssen, R. A. J.; Anthopoulos, T.; Siringhaus, H.; Heeney, M.; McCulloch, I. J. *J. Am. Chem. Soc.* **2011**, *133*, 3272.
- (14) Bürgi, L.; Turbiez, M.; Pfeiffer, R.; Bienewald, F.; Kirner, H.-J.; Winnewisser, C. *Adv. Mater.* **2008**, *20*, 2217.
- (15) Hao, Z.; Iqbal, A. *Chem. Soc. Rev.* **1997**, *26*, 203.
- (16) Braga, D.; Horowitz, G. *Adv. Mater.* **2009**, *21*, 1473.
- (17) Gao, Y.; Ma, P.; Chen, Y.; Zhang, Y.; Bian, Y.; Li, X.; Jiang, J.; Ma, C. *Inorg. Chem.* **2008**, *48*, 45.
- (18) Huettner, S.; Sommer, M.; Hodgkiss, J.; Kohn, P.; Thurn-Albrecht, T.; Friend, R. H.; Steiner, U.; Thelakkat, M. *ACS Nano* **2011**, *5*, 3506.
- (19) Lee, J.; Cho, S.; Seo, J. H.; Anant, P.; Jacob, J.; Yang, C. J. *Mater. Chem.* **2012**, *22*, 1504.
- (20) Chen, Z.; Lee, M. J.; Shahid Ashraf, R.; Gu, Y.; Albert-Seifried, S.; Meedom Nielsen, M.; Schroeder, B.; Anthopoulos, T. D.; Heeney, M.; McCulloch, I.; Siringhaus, H. *Adv. Mater.* **2012**, *24*, 647.
- (21) Zou, Y.; Gendron, D.; Neagu-Plesu, R.; Leclerc, M. *Macromolecules* **2009**, *42*, 6361.
- (22) Chen, L.; Deng, D.; Nan, Y.; Shi, M.; Chan, P. K. L.; Chen, H. J. *Phys. Chem. C* **2011**, *115*, 11282.
- (23) Huo, L.; Hou, J.; Chen, H.-Y.; Zhang, S.; Jiang, Y.; Chen, T. L.; Yang, Y. *Macromolecules* **2009**, *42*, 6564.
- (24) Mohebbi, A. R.; Yuen, J.; Fan, J.; Munoz, C.; Wang, M. F.; Shirazi, R. S.; Seifert, J.; Wudl, F. *Adv. Mater.* **2011**, *23*, 4644.
- (25) Mei, J.; Graham, K. R.; Stalder, R.; Tiwari, S. P.; Cheun, H.; Shim, J.; Yoshio, M.; Nuckolls, C.; Kippelen, B.; Castellano, R. K.; Reynolds, J. R. *Chem. Mater.* **2011**, *23*, 2285.
- (26) Burckstummer, H.; Weissenstein, A.; Bialas, D.; Würthner, F. *J. Org. Chem.* **2011**, *76*, 2426.
- (27) Kim, Y. H.; Park, S. K.; Moon, D. G.; Kim, W. K.; Han, J. I. *Jpn. J. Appl. Phys.* **2004**, *43*, 3605.
- (28) Ando, S.; Nishida, J.-i.; Tada, H.; Inoue, Y.; Tokito, S.; Yamashita, Y. *J. Am. Chem. Soc.* **2005**, *127*, 5336.
- (29) Ando, S.; Nishida, J.-i.; Fujiwara, E.; Tada, H.; Inoue, Y.; Tokito, S.; Yamashita, Y. *Chem. Lett.* **2004**, *33*, 1170.
- (30) Karikomi, M.; Kitamura, C.; Tanaka, S.; Yamashita, Y. *J. Am. Chem. Soc.* **1995**, *117*, 6791.
- (31) Lee, B.-L.; Yamamoto, T. *Macromolecules* **1999**, *32*, 1375.
- (32) Zhu, Y.; Champion, R. D.; Jenekhe, S. A. *Macromolecules* **2006**, *39*, 8712.
- (33) Osaka, I.; Sauv e, G.; Zhang, R.; Kowalewski, T.; McCullough, R. D. *Adv. Mater.* **2007**, *19*, 4160.
- (34) Al-Hashimi, M.; Baklar, M. A.; Colleaux, F.; Watkins, S. E.; Anthopoulos, T. D.; Stingelin, N.; Heeney, M. *Macromolecules* **2011**, *44*, 5194.
- (35) Smith, J.; Zhang, W.; Sougrat, R.; Zhao, K.; Li, R.; Cha, D.; Amassian, A.; Heeney, M.; McCulloch, I.; Anthopoulos, T. D. *Adv. Mater.* **2012**, *24*, 2441.